Morphology- and Mass-Dependent Galaxy Clustering and Luminosity Function Evolution

Patrick B. Hall

Galaxy clustering and luminosity function (LF) parameters are strong functions of morphology at z=0, with late-type galaxies being less strongly clustered and having a steeper faint-end LF slope than early-type galaxies, which are typically more massive. The redshift evolution of these quantities is known only sketchily, but they are key parameters since clustering evolution constrains structure formation theories and LF evolution constrains the evolution of galaxy populations. Realizing these constraints requires identifying the same galaxy populations at all redshifts, and morphological selection is better than color selection for this purpose since it is less biased by recent star formation. Using morphological galaxy classifications from *HST* for 5500 galaxies with known redshifts (4600 with R<21.5) from the Canadian Network for Observational Cosmology field galaxy redshift survey (CNOC2), I propose to determine galaxy clustering and LF evolution as a function of morphology out to z$\sim$0.6, and to begin the same determination as a function of dynamical mass using Keck. The morphological sample size is a $\geq$10$\times$ increase over previous studies and can be obtained in 212 *HST* orbits using the Advanced Camera for Surveys (ACS) Wide Field Camera.

Luminosity Function and Population Evolution

At z<0.05, LFs depend on morphology in the sense that early-type galaxies have a brighter M^* and a shallower faint end slope α than the typically less massive late-type galaxies (12; 16; 15; 14). Even with a steep faint-end slope for late-type galaxies, evolution is required to explain the excess of faint blue galaxies at moderate redshifts; there are many more L>L^* irregulars at z=0.6 than at z=0. The current best determination of morphologically dependent LFs at z>0.1 comes from *HST* data on $\sim$300 CFRS/LDSS galaxies (2; 24). These data are consistent with no density evolution and passive luminosity evolution for E/S0s and spirals and strong luminosity or density evolution (or both) for irregulars (Fig. 1a).

In CNOC2, the luminosity functions (LFs) of different galaxy SED (spectral energy distribution) types show different redshift evolution in the range 0.1<z<0.55 (Fig. 1b). Using SED types defined by fits of *UBVRI* colors to synthetic colors computed from the SEDs of (4), (10) finds nearly pure luminosity evolution for early (30% by number) and intermediate (25%) types and nearly pure number density evolution for late types (45%). This *description* of the LF evolution still requires linkage with the physical drivers of galaxy luminosity and density evolution, namely passive stellar evolution, mergers, and star formation and the processes which affect it (e.g. interactions/mergers, gas accretion, and secular bar, bulge, and disk creation and growth). Also, understanding galaxy LF evolution using different SED types is fundamentally limited by the frequency with which galaxies change their SED types, which might be high since a very small amount of star formation can dominate a galaxy's spectrum.

LF analyses divided by size, objective morphological classification, and other quantitative morphological parameters determined from *HST* imaging at λ_{rest}=0.5-0.8μm will be more physically meaningful as morphology is less easily affected by star formation than SED type.

The addition of morphologies to the CNOC2 database of redshifts, *UBVRIJK* magnitudes, SED types and spectral parameters will provide the means to link the observed evolution of galaxies with its physical underpinnings by identifying the same galaxy populations at different redshifts. This approach is limited by the movement of galaxies between different morphological classes, but these data will constrain such evolution as well. Besides estimates of space density evolution from LFs and V/V_{max} tests and simple counts of e.g. barred spirals with redshift, this survey will provide counts of very close pairs, interactions/mergers, and recent merger remnants impossible to identify from the ground. These can be used along with dynamical pairs (17) to find the galaxy merger and interaction rates from z=0.1-0.65.

These constraints will help gauge the limitations of morphological selection, but to overcome them will require mass-selected samples. Dynamical mass estimates can be obtained from spectroscopic line widths (13; 8) or rotation curves (25; 26), but they are much more expensive to obtain than morphologies. However, *HST* imaging provides the galaxy inclinations and orientations needed to begin gathering mass estimates, and with the dual-beam LRIS, DEIMOS, and ESI spectrographs available at Keck it is feasible to begin dynamical mass studies at z<0.7 (complementing the DEEP project at z>0.7) by targeting a few interesting subsamples. For example, studying the bluest galaxies over z=0.1-0.65 from a single data set sidesteps the need for a local comparison sample and should prove or disprove the hypothesis that at higher z such galaxies are typically less massive at fixed luminosity (13).

Work with WFPC2 has shown that the fraction of irregular and peculiar galaxies increases dramatically to higher redshifts and fainter apparent magnitudes (6), but mostly at I>21. The R<21.5 CNOC2 sample is well suited to define the evolution occuring in spiral and elliptical populations at moderate redshifts: 850 irregular, 2300 spiral, and 1450 E/S0 galaxies with redshifts are expected (5; 6), enough to also determine the SED type- and morphology-density relationships and their evolution with z in structures up to poor clusters in richness. In the irregular sample, $L>L^*$ examples (rare at z<0.6) will be studied and the evolution to $z\sim$0.6 of their LF, colors, and morphological parameters such as asymmetry will constrain how low and high redshift irregulars are related. Smaller galaxies may be responsible for most of the galaxy LF evolution at z<1 (9; 13); this sample will confirm or refute this.

With regard to spirals, (20), (9), and (19) find that disks had surface brightnesses $\sim$1^m brighter at $z\sim$1. However, (23) claims that this is primarily a selection effect, and that surface brightnesses were <0$^{\rm m}_{\cdot}$5 brighter at $z\sim$1, consistent with Tully-Fisher studies of a few $z\sim$1 disk systems (25; 26). Our large sample will enable construction of carefully defined subsamples which still contain large numbers of galaxies; this will be a great help in improving our understanding of disk surface brightness evolution as well as many other issues.

As for ellipticals, (21) presented a sample of 46 E/S0s with redshifts from *HST* imaging of the CFRS, in which they find ΔM_B=–1 and $\Delta(U-V)$=–0.7 since $z\sim1$. The expected number of E/S0 galaxies in the CNOC2 sample is sufficient to repeat this study in ∼23 redshift bins. (21) find evidence that the dispersion in color among $z\sim0.55$ field E/S0s may be larger than among $z\sim0.55$ cluster E/S0s; this sample will track the evolution of the color dispersion, color, and surface brightness in the field from z=0.1–0.55 and enable comparison of isolated E/S0s with group members. (21) find 1/3 of E/S0s have [O II] emission; this sample will track the evolution of this fraction (and its correlation with broad-band color) with z. (21) find no evidence for a change in the space density of ellipticals at $z<1$; this E/S0 sample will be large enough to measure V/V_{max} with an uncertainty 5× lower than theirs and detect a 20% change in the space density of such galaxies between z=0.1–0.65 at the 1σ level.

Clustering Evolution

Large-scale galaxy clustering studies aim to understand the underlying mass distribution and the bias(es) of galaxies relative to it. Because of bias, it is crucial to identify the same galaxy population at all redshifts. In an important step toward this, (3) compile an evolution- and k-corrected volume-limited sample of ∼2500 luminous ($M_R<-20$) CNOC2 galaxies and find that the correlation length r_0 of such galaxies remains roughly fixed in comoving coordinates to $z\sim0.65$ — i.e., the density of luminous galaxies within 0.1–10h^{-1} Mpc of themselves is approximately constant to $z\sim0.65$. Using the same sample, (22) show that early SED type galaxies are more strongly clustered than intermediate and late SED types from z=0.1–0.65, as seen at $z\sim0$ (11; 7; 27). However, (22) also show that the redshift evolution of clustering is a strong function of galaxy SED type (Fig. 2). Late SED types show a moderate increase in comoving r_0 from $z\sim0.6$ to $z\sim0.2$, but early and intermediate SED types show a ∼50% decrease in r_0, implying an unphysical disappearance of 5h^{-1} Mpc scale structures over a few Gyr. This can be explained by a population of galaxies (early-type spirals?) reddening and moving to earlier SED types with time, thus lowering the observed r_0 for such SED types.

This hypothesis will be tested using morphology-defined samples and incorporating morphology-dependent evolution corrections. These will be compared with morphology-blind samples to determine the latter's suitability for clustering evolution studies. This will be the first study of morphology-dependent clustering at $z>0.1$. The redshift evolution of r_0 as a function of size and morphology, of the relative bias of different populations on 0.1–10h^{-1} Mpc scales (27) and of the strength of luminosity and morphological segregation on the same scales will constrain theories of biased galaxy formation and test the suggestion that luminosity segregation is primordial while morphological segregation is enhanced by environmental factors (11).

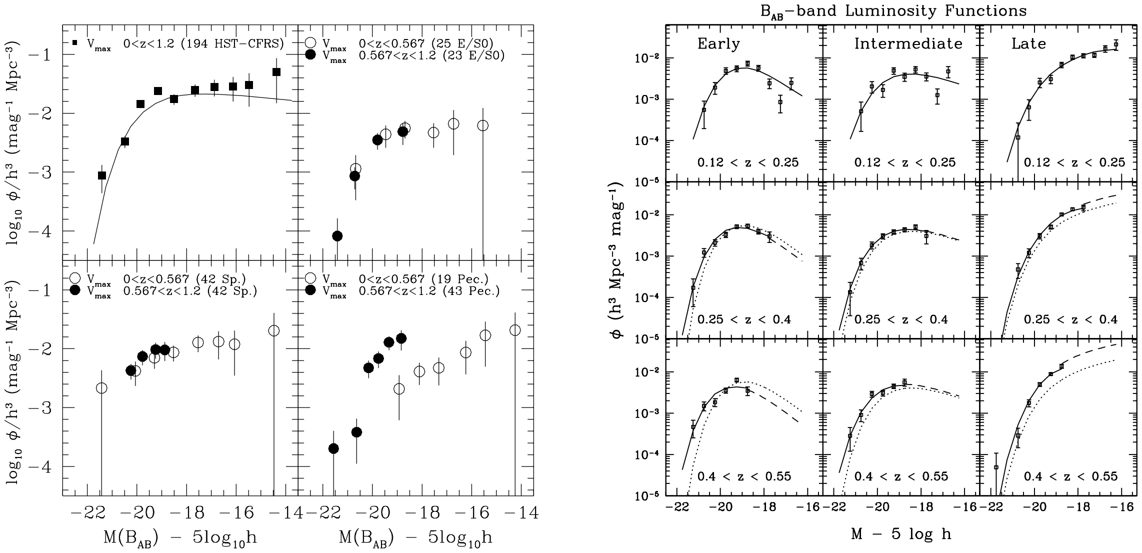

Fig. 1.— a. Canada-France Redshift Survey/Low-Dispersion Survey Spectrograph total and morphologically divided LFs (24), the best currently available at $z \geq 0.1$. b. CNOC2 LFs divided by SED-type (10); this proposal will yield an equivalent plot divided by morphology. Note that *each column of b.* would correspond to *just the filled points in a.* for each morphological type, illustrating this proposal's gain over existing data at $z < 0.6$.

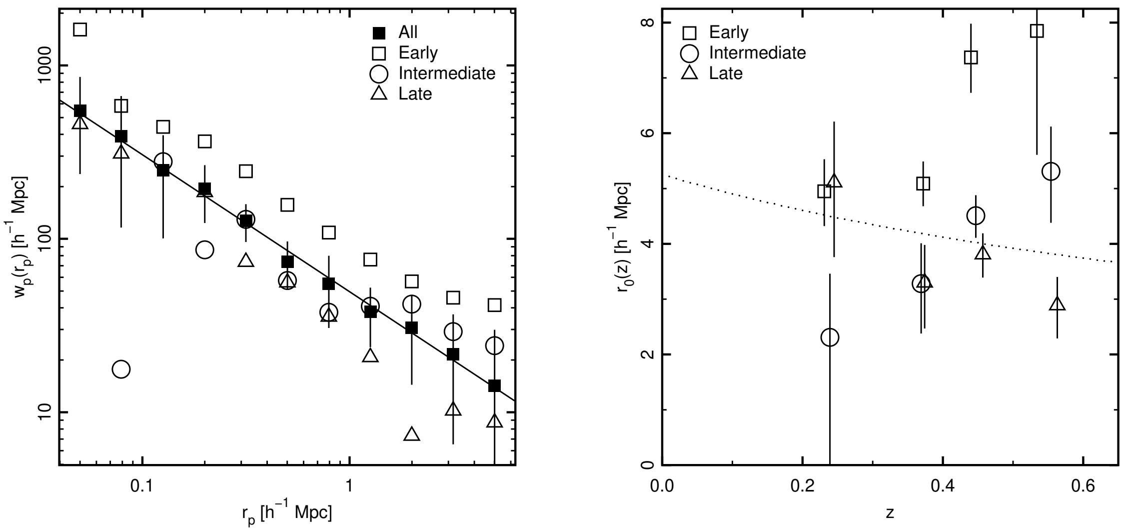

Fig. 2.— From (22). a. The projected two-point correlation function ω_p as a function of co-moving projected separation r_p for the entire CNOC2 high-luminosity subsample and for each SED class. b. Co-moving correlation length r_0 as a function of redshift for each SED class (points) and the fit to all SEDs (dotted line).

Technical Considerations

Morphological parameters will be measured using quantitative methods developed for WFPC2 (1; 18; 21). The science requires contiguous imaging to minimize the noise in clustering analyses. Optimal ACS tiling covers 88.5% of CNOC2, yielding $\sim$5480 galaxies with redshifts ($\sim$4600 with R<21.5). Two pointings per orbit gives exposures of 750s (ACS) and 870s (WFPC2) per pointing. From (18), 99.7% of R<21.5 galaxies should be classifiable in an 870s WFPC2 F814W image, and the limit should be $\sim 1^m$ fainter with ACS despite smaller pixels, lessening the sensitivity to $(1+z)^4$ surface brightness dimming (ACS Mini-Handbook, 1999).

REFERENCES

1. Abraham, R. G., *et al.* 1996, ApJS, 107, 1
2. Brinchmann, J., *et al.* 1998, ApJ, 499, 112
3. Carlberg, R. G., *et al.* 1999, submitted to ApJ
4. Coleman, G. D., Wu, C.-C., & Weedman, D. W. 1980, ApJS, 43, 393
5. Cowie, L. L., Hu, E. M., & Songaila, A. 1995, AJ, 110, 1576
6. Driver, S. P., Windhorst, R. A., & Griffiths, R. E. 1995, ApJ, 453, 48
7. Hermit, S., *et al.* 1996, MNRAS, 283, 709
8. Kelson, D., *et al.* 1999, ApJ, in press (astro-ph/9908257)
9. Lilly, S., *et al.* 1998, ApJ, 500, 75
10. Lin, H., *et al.* 1999, ApJ, 518, 533
11. Loveday, J., Maddox, S. J., Efstathiou, G., & Peterson, B. A. 1995, ApJ, 442, 457
12. Loveday, J., Peterson, B. A., Efstathiou, G., & Maddox, S. J. 1992, ApJ, 390, 338
13. Mallen-Ornelas, G., Lilly, S. J., Crampton, D., & Schade, D. 1999, ApJ, 518, L83
14. Marinoni, C., Monaco, P., Giuricin, G., & Costantini, B. 1999, ApJ, 521, 50
15. Marzke, R. O., *et al.* 1998, ApJ, 503, 617
15. Marzke, R. O., Geller, M. J., Huchra, J. P., & Corwin, Harold G., J. 1994, AJ, 108, 437
17. Patton, D. R., *et al.* 1999, in preparation
18. Ratnatunga, K. U., Griffiths, R. E., & Ostrander, E. J. 1999, AJ, 118, 86
19. Roche, N., Ratnatunga, K., Griffiths, R., Im, M., & Naim, A. 1998, MNRAS, 293, 157
20. Schade, D., *et al.* 1996, ApJ, 465, L103
21. Schade, D., *et al.* 1999, in press (astro-ph/9906171)
22. Shepherd, C. W., to appear in "Clustering at High Redshift"
23. Simard, L., *et al.* 1999, ApJ, 519, 563
24. Tresse, L. 1999 (astro-ph/9902209)
25. Vogt, N. P., *et al.* 1996, ApJ, 465, L15
26. Vogt, N. P., *et al.* 1997, ApJ, 479, L121
27. Willmer, C. N. A., Da Costa, L. N., & Pellegrini, P. S. 1998, AJ, 115, 869

28. Clampin, M., *et al.* 1999, Advanced Camera for Surveys Mini-Handbook

---